PHYSICAL REVIEW B **68**, 241405(R) (2003)

Microscopic theory for nanotube piezoelectricity

Na Sai and E. J. Mele
Department of Physics and Astronomy, University of Pennsylvania, Philadelphia, Pennsylvania 19104, USA
(Received 21 August 2003; published 31 December 2003)

We combine *ab initio*, tight-binding methods and analytical theory to study piezoelectric effect of boron nitride nanotubes. We find that piezoelectricity of a heteropolar nanotube depends on its chirality and diameter and can be understood starting from the piezoelectric response of an isolated planar sheet, along with a structure specific mapping from the sheet onto the tube surface. We demonstrate that a linear coupling between the uniaxial and shear deformation occurs for chiral nanotubes. Our study shows that piezoelectricity of nanotubes is fundamentally different from its counterpart in three-dimensional bulk materials.

DOI: 10.1103/PhysRevB.68.241405 PACS number(s): 73.22.−f, 77.65.−j

The physical properties of a nanotube along its extended direction are controlled by the boundary conditions imposed along its wrapped direction. The existence of both semiconducting and metallic forms of pure carbon nanotubes provides a striking example.[1] The recently discovered electric polarization in heteropolar nanotubes (e.g., boron nitride) presents a new physical manifestation of this effect.[2] Since the polarization can be modulated by elastic strains of the tube, these materials provide a new class of *molecular piezoelectrics* where mechanical strain is linearly coupled to an electric field. Piezoelectric nanotubes thus hold promise for application in nanometer scale sensors and actuators.

In the modern quantum theory of polarized solids the electric polarization is computed from the geometric phase[3] (Berry phase) accumulated by the occupied electronic states as one introduces a potential that adiabatically connects an unpolarized and a polarized state of the system. For a BN nanotube the Berry phase and hence the polarization is controlled by the periodic boundary condition on electronic wave functions.[2] The piezoelectric effect, on the other hand, is determined by the dependence of macroscopic polarization on the local strain induced effects: redistribution of the valence charge density, curvature induced rehybridization of the electronic orbitals, and relaxations of the positions of the atoms on the tube walls which are all short range in character. Here we show that it is this latter character that allows the piezoelectric response to follow a simple transformation rule when the structure changes from a sheet to tube geometry.

The prototypical example of piezoelectric nanotubes is found in the family of BN nanotubes where the alternation of group III(B) and group V(N) elements on the honeycomb lattice lowers the symmetry. A BN nanotube can have a nonzero electric polarization[4] unlike its planar counterpart where this is forbidden by the threefold rotational symmetry of an isolated two-dimensional (2D) BN sheet. However an elastic coplanar deformation of a BN sheet lowers its lattice symmetry, redistributes the valence charge, and produces a nonzero polarization. Figure 1 illustrates the effect of a uniaxial strain (η_{xx}) and a shear strain (η_{yx}) of the BN sheet, with both distortions greatly exaggerated for clarity. These distortions induce the electric dipole moments denoted by the arrows. The linear response of the electric polarization P_i to an applied strain η_{jk} is described by the third rank piezoelectric tensor $e_{ijk}=\partial P_i/\partial \eta_{jk}$. The $3m$ symmetry of the unstrained sheet requires that the piezoelectric tensor be unchanged by threefold rotations of the lattice and the elements of the piezoelectric tensor obey the symmetry relation $e_{xxx}=-e_{xyy}=-e_{yxy}=-e_{yyx}$.

To study the microscopic origin of this behavior we first carried out *ab initio* calculations of the piezoelectric constants of the flat BN sheet using a plane-wave pseudopotential method based on density-functional theory (DFT) within the local-density approximation. The calculation is performed with the ABINIT package[5] using Troullier-Martins pseudopotentials[6] with an energy cutoff of 45 hartree and $4\times4\times1$ k-point grid throughout. To create a computational cell that is periodic in all three spatial dimensions we stacked the BN sheets with an interplanar distance 20 bohrs so that there is negligible wave-function overlap between layers. The electronic polarization was computed for a series of strained lattices using the Berry phase formulation[3] (discretized on a dense k-point grid along the direction of the polarization) and the piezoelectric constants were obtained by calculating lattices with strains in the range of $1\%\leqslant\eta_{jk}\leqslant5\%$. By defining the positive direction to be the bond direction from N atom to B atom as shown in Fig. 1, we find

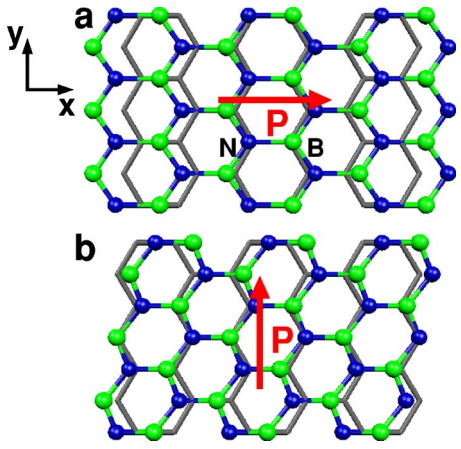

FIG. 1. (Color online) BN flat sheets under uniaxial strain η_{xx} (a) and shear strain η_{xy} (b). In both cases, threefold symmetry is broken and charge redistribution gives rise to a net dipole moment. The corresponding polarization directions (P) are marked by arrows.

$e_{xxx}=0.12\ e$/bohr. Our calculations for the sheets with a shear strain η_{xy} have explicitly verified the symmetry relations among the piezoelectric tensor elements and showed that the piezoelectric properties of the sheet are controlled by a single coefficient. To carry out a systematic study of the piezoelectric behavior of a large family of wrapped structures parametrized by integer indices (m,n),[1] we combine the *ab initio* DFT method with a computationally less intensive albeit less accurate tight-binding (TB) method. We used a nonorthogonal basis set with four orbitals per site to describe the $2s$ and $2p$ atomic orbitals.[7] We were able to benchmark our tight-binding method by comparing calculations of the piezoelectric constant of the BN sheet using both theories. We find that the TB theory yields $e_{xxx}=0.086\ e$/Bohr which is smaller than the *ab initio* result, though in acceptable agreement.

Note that the piezoelectric constants of a 2D BN sheet have the dimensions of charge per unit length. A quantitative comparison of the piezoelectric constants of the flat sheet to the piezoelectric coefficients of three-dimensional (3D) bulk material requires specification of the interlayer spacing and packing. For example, if we convert the above 2D flat sheet value into a conventional ''bulk'' piezoelectric constant for a hypothetical 3D bulk material using the primitive interlayer separation of 0.34 nm,[8] we find $e_{3D}=0.76$ C/m^2. In comparison, this value is similar in magnitude to $e_{33}=0.73$ C/m^2 of wurtzite nitrides (e.g., GaN) (Ref. 9) and is larger than 0.12 C/m^2 of piezoelectric polymer polyvinylidene fluoride[10] which are both commonly used piezoelectric materials. Alternatively the piezoelectric constant computed from different dimensional system can be expressed as total dipole per stoichiometric unit. Using this convention, we find that the piezoelectric constant is 1.67 dipole/unit for the BN sheet, smaller than 1.98 dipole/unit for GaN wurtzite. As we show below, when a sheet is wrapped to form a tube, the piezoelectric constants of a given tube can be computed from the piezoelectric constants for the flat sheet.

Two high-symmetry families of nanotubes are the zigzag structures with wrapping indices $(n,0)$ and the armchair structures with wrapping indices (n,n). The one-dimensional (1D) piezoelectric constants are defined as $e_{11}=\partial P_z/\partial\eta_s$ and $e_{14}=\partial P_z/\partial\eta_t$, where P_z is the dipole moment per unit length and the (z,s,t) indices in the tube frame refer, respectively, to the tube axis z, the uniaxial s, and torsional t strains. In Fig. 2, the top panel shows the structures of two representative small radius members of each family and in the bottom panel we plot their piezoelectric constants in unit comparable with the two-dimensional piezoelectric constants. Note that the 1D piezoelectric constant is proportional to the tube circumference C through $e_{1D}=C\,e_{2D}$. We find that zigzag tubes exhibit a longitudinal piezoelectric response for the case of uniaxial strain (extension or compression) but not for torsion. In contrast the armchair tubes have an electric dipole moment linearly coupled to torsion, but not to a uniaxial strain. The complementary strains, i.e. torsion for the zigzag structures and stretch for the armchair structures, produce a purely azimuthal dipole that integrates to zero on the surface of the cylinder.

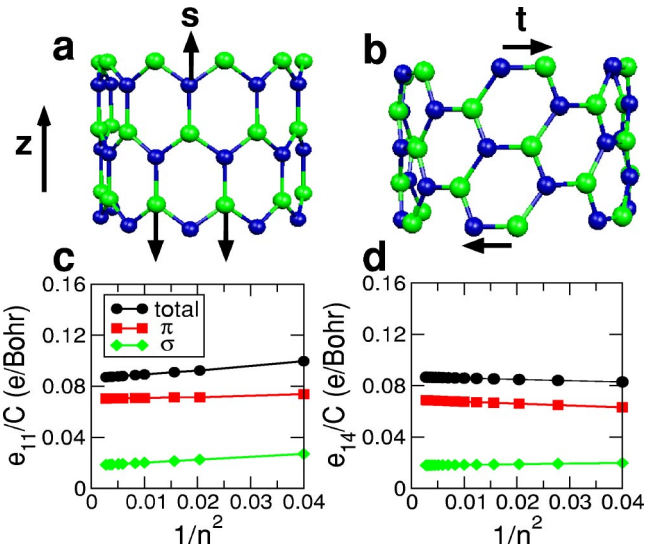

FIG. 2. (Color online) Schematic structures of (a) stretched $(n,0)$ nanotubes and (b) twisted (n,n) nanotubes where arrows display the strain deformation direction in the tangential plane. Panels (c) and (d) show the calculated tube piezoelectric constant e_{11}/C and e_{14}/C as functions of $1/n^2$, where C is the tube circumference. Contributions from σ and π electrons to the total piezoelectric response are separated.

For large radius tubes, one expects a correction to the piezoelectric constants of tube from its curvature, proportional to the inverse square of the tube radius. This can be seen in Fig. 2 bottom panel where we quantify this scaling behavior by plotting the calculated piezoelectric constants as a function of $1/n^2$. The data show that the tube piezoelectric constant rapidly approaches the flat sheet values with this scaling relation, but also that curvature effects remain quite small even for relatively small radius tubes. The data also show that contribution to the piezoelectric response from the π and σ valence electrons have the same sign for both families of structures, with the π electrons dominating the piezoelectric response, accounting for $\approx 80\%$ of the total.

For a chiral tube the wrapping vector does not lie along a high-symmetry direction of the 2D honeycomb lattice. This leads to a large and low symmetry translational unit cell for the chiral nanotube making a direct calculation of its piezoelectric properties cumbersome. We make use of the results for the high-symmetry armchair and zigzag structures to develop an accurate scaling theory of the piezoelectric response of chiral tubes. Ignoring the finite radius corrections arising from the tube curvature the elements of the piezoelectric tensor are specified by rotating the known piezoelectric elements of the flat sheet onto the symmetry axes of the tube. Thus, defining the chiral angle θ as the angle between the axis of the tube and a 2D primitive translation vector we find

$$e_{11}=C\,e_{xxx}\sin(3\theta),$$

$$e_{14}=C\,e_{yxy}\cos(3\theta). \qquad (1)$$

Finite radius corrections to the predictions of Eq. (1) can then be obtained by comparing the results of this mapping to

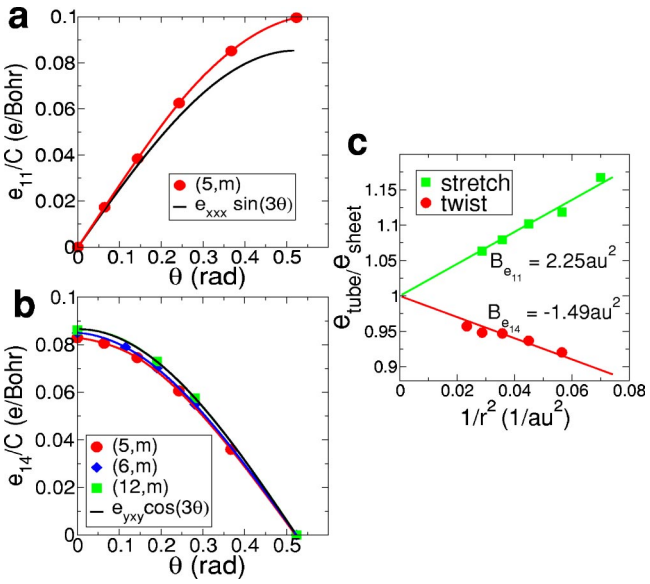

FIG. 3. (Color online) Piezoelectric response as function of the chiral angle in a sample of chiral nanotubes experiencing the uniaxial strain (a) and the shear strain (b). Solid black curves are the analytical result, Eq. (1). Panel (c) shows ratio of the piezoelectric constants of chiral nanotubes, e_{tube}, to their flat sheet values e_{sheet} plotted as a function of the inverse square radius. The two branches are for the uniaxial e_{11} and torsional e_{14} response.

the values obtained from TB calculations on a selected set of chiral structures. Figures 3(a) and 3(b) show the result of this comparison, for uniaxial strain on the family of $(5,m)$ tubes and for torsion on the families of $(5,m)$, $(6,m)$, and $(12,m)$ families, respectively. These data are very well described by the mapping of the 2D results, with surprisingly small corrections due to the tube curvature. The correction is quantified in Fig. 3(c) where we plot the ratio of the calculated piezoelectric modulus to its flat sheet $(n\rightarrow\infty)$ value as a function of $1/r^2$ for the family of $(5,m)$ tubes. The ratio is well approximated by the form $1+B/r^2$ where B is a parameter. Our fitted values of the parameters B are indicated in the figure. The deviations from the predictions of the flat sheet model are less than 15% over the entire range of structures we studied.

Equation (1) also reveals that the chiral tube has allowed linear piezoelectric coupling to both uniaxial strain *and* torsion, unlike the higher-symmetry zigzag or armchair structures. Thus the long-wavelength elastic energy of a chiral tube generically has an anomalous cross term containing the product of the uniaxial and torsional strains. This implies that a tensile stress applied to a chiral tube induces torsion and conversely torsion induces a change of its length. Such a coupling is only possible for a chiral molecular structure, and indeed the coefficient of the cross term is a macroscopic manifestation of the underlying microscopic chirality of the nanotube.

Recent progress in the synthesis of nanoscale materials is demonstrating that many three-dimensional lamellar phases can be fabricated in compact cylindrical structures.[11] The appearance of pyroelectric and piezoelectric effects is a generic feature of these structures, and can be excluded only for special high-symmetry wrappings. The methods we have developed and tested here for BN nanotubes should be widely applicable to study piezoelectric effects in this broader family of nanoscale materials.

This work was supported by Department of Energy under Grant No. DE-FG02-ER0145118 and by National Science Foundation under Grant No. DMR-00-79909. We thank J. Bernholc, S. Nakhmanson, and P. Lammert for helpful discussions.

[1] M.S. Dresselhaus, G. Dresselhaus, and P.C. Eklund, *Science of Fullerences and Carbon Nanotubes* (Academic, San Diego, 1996).

[2] E.J. Mele, and P. Kráľ, Phys. Rev. Lett. **88**, 056803 (2002).

[3] R.D. King-Smith and D. Vanderbilt, Phys. Rev. B **47**, 1651 (1993).

[4] The electronic contribution described by the Berry phase is partially compensated by a dipole from the fixed ionic charges on the honeycomb lattice sites. In the limit of a strongly ionic system, these two contributions nearly cancel [S.M. Nakhmanson, A. Calzolari, V. Meunier, J. Bernholc, and M. Buongiorno-Nardelli, Phys. Rev. B **67**, 235406 (2003)].

[5] X. Gonze *et al.*, Comput. Mater. Sci. **25**, 478 (2002).

[6] N. Troullier and J.L. Martins, Phys. Rev. B **43**, 1993 (1991).

[7] J. Widany, Th. Frauenheim, Th. Köhler, M. Sternberg, D. Porezag, G. Jungnickel, and G. Seifert, Phys. Rev. B **53**, 4443 (1996).

[8] J.P. Lu, Phys. Rev. Lett. **79**, 1297 (1997).

[9] F. Bernardini, V. Fiorentini, and D. Vanderbilt, Phys. Rev. B **56**, R10 024 (1997).

[10] V.V. Kochervinskiĭ, Crystallogr. Rep. **48**, 649 (2003).

[11] R. Tenne and A.K. Zettl, Top. Appl. Phys. **80**, 81 (2002).